 doi:10.20944/preprints202009.0529.v1

# Pre-operational Sentinel-3 Snow and Ice (SICE) Products

Algorithm Theoretical Basis Document

Version 3.1

September 22, 2020

A. A. Kokhanovsky (1), J. Box (2), B. Vandecrux (2)

(1) VITROCISET Belgium SPRL, Bratustrasse 7, 64293 Darmstadt, Germany

(2) Geological Survey of Denmark and Greenland (GEUS)
Øster Voldgade 10, 1350 Copenhagen, Denmark

 doi:10.20944/preprints202009.0529.v1

**Abstract:** This document describes the theoretical basis of the algorithms used to determine properties of snow and ice from the measurements of the Ocean and Land Color Instrument (OLCI) onboard Sentinel-3 satellites within the Pre-operational Sentinel-3 snow and ice products (SICE) project: http://snow.geus.dk/. The code used for the SICE retrieval and its documentation can be found at https://github.com/GEUS-SICE/pySICE. The algorithms were developed after the work from Kokhanovsky et al. (2018, 2019, 2020).

**Keywords:** snow; albedo; remote sensing; OLCI; Sentinel-3

---

Preprints (www.preprints.org) | NOT PEER-REVIEWED | Posted: 23 September 2020 doi:10.20944/preprints202009.0529.v1

## 1. Introduction

This document describes the theoretical basis of the algorithms used to determine properties of snow and ice from the measurements of the Ocean and Land Color Instrument (OLCI) onboard Sentinel-3 satellites within the Pre-operational Sentinel-3 snow and ice products (SICE) project: http://snow.geus.dk/. The code used for the SICE retrieval and its documentation can be found at https://github.com/GEUS-SICE/pySICE. The algorithms were developed after the work from Kokhanovsky et al. (2018, 2019, 2020a).

Snow is composed of ice crystals in contact with each other and surrounded by air. Snow can include impurities such as dust, soot, algae (e.g., Skiles et al., 2018), here referred to as 'pollution'. Snow can also contain liquid water. The volume concentration of snow grains is usually around 1/3 with 2/3 of the snow volume occupied by air (Proksch et al., 2016). The concentration of pollutants is often low, that is, below 100 ng/g especially in polar regions (Doherty et al., 2010).

The algorithms described here are dedicated to the retrieval of snow optical properties such as snow spectral and broadband albedo and also snow microstructure (snow specific surface area and effective optical grain size). We propose a snow mask based on the Normalized Difference Snow Index (NDSI) and a technique to retrieve the concentration of pollutants in snow, which is possible only for the cases with relatively heavy (above 1ppmv) pollution load (Warren, 2013).

### 1.1. Ocean and Land and Colour Instrument

Ocean and Land and Colour Instrument (OLCI) is a 21 band spectrometer that measures solar radiation reflected by the Earth's atmosphere and surface with a ground spatial resolution of 300 m (see Table 1). The OLCI swath width is 1270 km. OLCI is installed on both Sentinel-3A and Sentinel-3B satellite platforms operated by the European Space Agency (ESA) in service to the European Union Copernicus Programme. The Sentinel-3 A and B orbit at 802 km altitude, 98.6 orbital inclination and a 10:00 UTC sun-synchronous equatorial crossing time.

Preprints (www.preprints.org) | NOT PEER-REVIEWED | Posted: 23 September 2020 doi:10.20944/preprints202009.0529.v1

***Table 1. Band characteristics of the Sentinel-3 Ocean and Land Colour Instrument (OLCI)[1]***

| Band | λ centre (nm) | Width (nm) | Band | λ centre (nm) | Width (nm) | Band | λ centre (nm) | Width (nm) |
|---|---|---|---|---|---|---|---|---|
| 1 | 400 | 15 | 8 | 665 | 10 | 15 | 767.5 | 2.5 |
| 2 | 412.5 | 10 | 9 | 673.75 | 7.5 | 16 | 778.75 | 15 |
| 3 | 442.5 | 10 | 10 | 681.25 | 7.5 | 17 | 865 | 20 |
| 4 | 490 | 10 | 11 | 708.75 | 10 | 18 | 885 | 10 |
| 5 | 510 | 10 | 12 | 753.75 | 7.5 | 19 | 900 | 10 |
| 6 | 560 | 10 | 13 | 761.25 | 2.5 | 20 | 940 | 20 |
| 7 | 620 | 10 | 14 | 764.375 | 3.75 | 21 | 1 020 | 40 |

### 1.2. Generated Products

The products of the SICE algorithms are listed in Table 2. Most of retrievals are based on the measurements at 865 and 1020nm, where the influence of atmospheric light scattering and absorption processes on top-of-atmosphere signal as detected on a satellite over polar regions is weak.

***Table 2. SICE: Snow and ice products***

| | Snow product name | Related Section | Units | Expected range | Maximum acceptable uncertainty in modelling | Optimum uncertainty |
|---|---|---|---|---|---|---|
| 1 | Snow mask | ***NDSI and NDBI*** | - | 0, 1 | <10% | 5 % |
| 2<br>3<br>4 | Spectral spherical snow albedo<br>Spectral planar snow albedo<br>Spectral surface reflectance | ***Retrieval of the surface characteristics*** | - | 0 -1.0 | <10% | 5 % |
| 5 | Broadband snow albedo (planar and spherical, for three spectral ranges) | ***Broadband albedo calculation*** | - | 0-1.0 | <15%* | <5%* |
| 6 | Snow Specific Surface Area | ***Clean snow*** | $m^2$ $kg^{-1}$ | 20-200 | <15% | 5 % |
| 7 | Snow grain diameter | ***Clean snow*** | mm | 0.02-0.2 mm | <15% | 5 % |
| 8 | Type and concentration of pollutants | ***Pollutant characteristics*** | ppmv ($10^{-6}$) | 0.1-10.0 | - | - |
| 9<br>10 | Normalized difference snow index<br>Normalized difference bare ice index | ***NDSI and NDBI*** | - | - | - | - |

* Source: GCOS (WMO, 2011)

[1] *https://sentinel.esa.int/web/sentinel/user-guides/sentinel-3-olci/resolutions/radiometric*

Preprints (www.preprints.org) | NOT PEER-REVIEWED | Posted: 23 September 2020 doi:10.20944/preprints202009.0529.v1

### 1.3. Summary of assumptions

The simplified snow layer model represents snow as a:

1. Horizontally homogeneous plane parallel turbid medium;
2. Vertically homogeneous layer;
3. Semi-infinite layer. Therefore, there is no need to account for the reflective properties of underlying surface.
4. Close packed effects are ignored.
5. Geometrical optics can be used to derive local optical snow characteristics.
6. Impurities (dust, soot, etc.) are located external to ice grains.
7. The single light scattering angular pattern is spectrally neutral in the spectral range given in Table 1.
8. Only pixels completely covered by snow are considered, i.e., pixels with ice and/or partially snow pixels are ignored.
9. The effects of slopes and snow roughness are not accounted for.

The output is provided if the OLCI reflectance at 1020nm is larger than 0.1 and the derived diameter of grains is larger than 0.1mm.

## 2. Snow and ice property retrievals

### 2.1. Definitions

#### 2.1.1. Geometry of the system

Preprints (www.preprints.org) | NOT PEER-REVIEWED | Posted: 23 September 2020 doi:10.20944/preprints202009.0529.v1

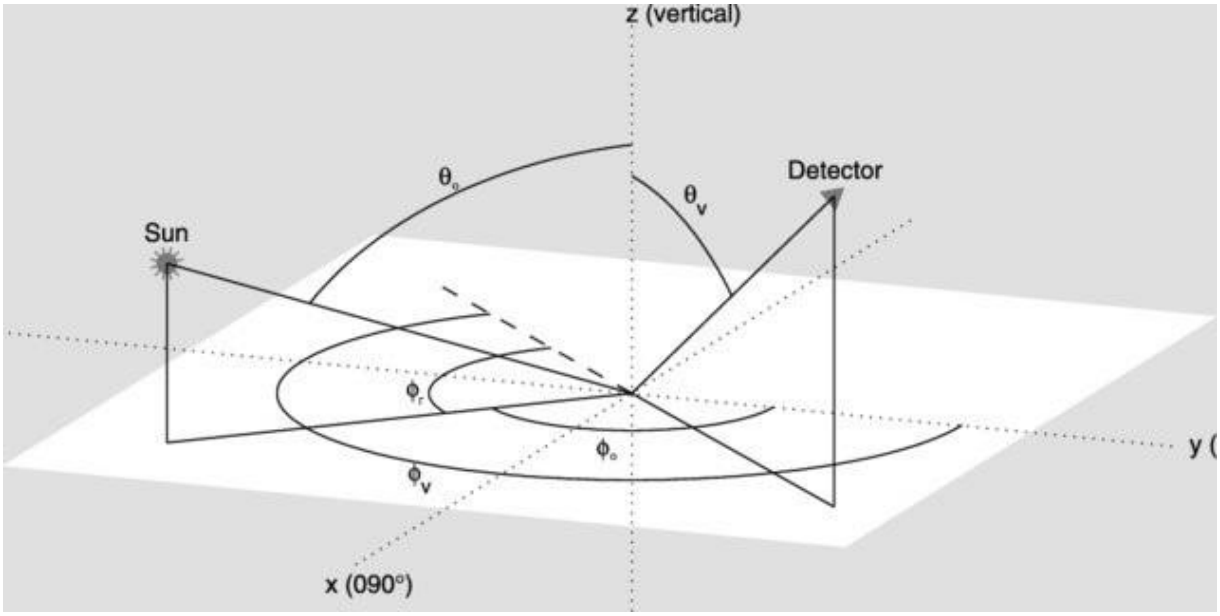


***Figure 1. Definition of the solar zenith angle $\theta_0$, azimuth angle $\phi_0$, viewing zenith angle $\theta_v$ and relative azimuth angle $\phi_r$. Illustration adapted from Hudson et al. (2006).***

The angles describing the solar and satellite positions around the point observation are presented in Figure 1. From these we derive the cosine of the solar zenith angle $\mu_0$, the cosine of the viewing zenith angle $\mu$ and the scattering angle $\theta$ :

$$\mu_0 = \cos\ \theta_0, \tag{2.1.1}$$
$$\mu = \cos\theta_v\ ,$$
$$cos\ \theta\ = -cos\ \theta_0 \cos\theta_v + \sin\theta_0 \sin\theta_v\ cos\ \phi_r$$

### 2.1.2. Reflectance, spherical and plane albedos

The **top-of-atmosphere reflectance** is defined as:

$$R_{TOA} = \frac{\pi I^{\uparrow}}{\mu_0 F_0}, \tag{2.1.2}$$

where, $I^{\uparrow}$ is the intensity of reflected light, $F_0$ is the solar flux at the top-of-atmosphere. Many satellite instruments simultaneously measure both $I^{\uparrow}$ and $F_0$ and allow the derivation of the top-of-atmosphere reflectance. In the absence of cloud, the **bottom-of atmosphere reflectance or snow reflectance $R_s$** is defined by Eq. (2.1.2) when applied at the bottom of the atmosphere.

Preprints (www.preprints.org) | NOT PEER-REVIEWED | Posted: 23 September 2020 doi:10.20944/preprints202009.0529.v1

The reflectance depends on atmospheric effects due to molecular and aerosol scattering and absorption of solar radiation. For retrieval of surface optical properties, these effects must be removed.

The ***plane albedo*** $\boldsymbol{r_p}$ is defined as the integration of bottom-of atmosphere reflectance $R$ across all viewing azimuth $\phi_v$ and zenith $\theta_v$ angles:

$$r_p(\mu_0) = 2\int_o^1 \frac{1}{2\pi}\int_0^\pi R(\mu_0, \mu_v, \phi_v) d\phi_v \ \mu_v d\mu_v, \quad (2.1.3)$$

The ***spherical albedo*** $\boldsymbol{r_s}$ is found by integration of $R$ over all incident angles $\theta_0$:

$$r_s = 2\int_o^1 \mathrm{R}(\mu_0)\mu_0 d\mu_0 \quad (2.1.4)$$

## 2.2. Retrieval overview

We first convert the top of the atmosphere radiance to reflectance using the SNAP Rad2Refl module. The top of the atmosphere reflectances $R_{TOA,}$ are then corrected for ozone and molecular scattering. Retrievals are thereafter approached in two ways, depending on whether they are considered as clean or polluted snow. The test differentiating these two snow conditions is based on the theory presented in Section ***Clean snow***: given the pixel's illumination and viewing geometry, we calculate the theoretical $R_{TOA}$ at band 1 ($\lambda$ = 400 nm) that this pixel would have if it had a surface reflectance of 1. If the observed $R_{TOA}$ is higher than this virtual $R_{TOA,}$ the pixel is considered as clean snow. Otherwise it is considered as polluted snow.

*Clean snow retrieval approach*

If the pixel is classified as clean snow, we derive snow spectral albedo in the spectral range 0.3-2.4 micrometres using the two-parameter analytical equation as described by Kokhanovsky et al. (2019) under assumption that atmospheric effects can be ignored at OLCI channels 16 and 21 ($\lambda$ = 865 nm and $\lambda$ = 1020 nm). This simple approach has produced good performance when comparing the retrieved snow spectral albedo and broadband albedo to ground observations (Kokhanovsky et al., 2019).

*Polluted snow retrieval approach*

The atmospheric correction for the polluted snow is treated in two ways depending on the OLCI reflectance at band 21 ($\lambda$ = 1020 nm).

Preprints (www.preprints.org) | NOT PEER-REVIEWED | Posted: 23 September 2020 doi:10.20944/preprints202009.0529.v1

*Case 1: Polluted pixels with $R_{TOA}$ at band 21 over 0.4*

If OLCI reflectance at channel 21 is above 0.4, we assume that scattering and absorption of light by surface impurities and atmosphere can be ignored at the wavelengths 865 and 1020nm but not below 865 nm. Therefore, reflectances of bands above 16 are being retrieved based on the OLCI measurements at bands 16 and 21 (λ = 865 nm and λ = 1020 nm) using the analytical equation for the spectral surface albedo presented by Kokhanovsky et al. (2019). For wavelengths below 865 nm, we account for gaseous absorption and light scattering by aerosol in the framework of the theory described in Section ***Atmospheric correction***.

*Case 2: Polluted pixels with $R_{TOA}$ at band 21 under 0.4*

In the case of polluted and dark ($R_{TOA}$ at band 21 under 0.4) snow and ice pixels, scattering within the atmosphere affect *all OLCI channels*. We can no longer assume that pollutants and other effects have small influence on OLCI reflectance above 865nm. Here we need an additional assumption on the intrinsic optical properties of these dark surfaces before the retrieval is performed.

In both cases, the albedo inside O2 and water vapor absorption bands is derived using the linear interpolation of results for neighbouring channels.

## 2.3. Atmospheric correction

### 2.3.1. Correction of the OLCI TOA reflectance for molecular absorption

The top-of-the-atmosphere reflectance $R_{TOA}$ is corrected for ozone absorption using the ozone transmittance function $T_{O_3}$:

$$R_{TOA,cor\,O_3}(\lambda) = R_{TOA}\,T_{O_3}(\lambda)\,, \tag{2.3.1}$$

Where the transmittance function is defined as in Rozanov and Rozanov (2010):

$$T_{O_3}(\lambda) = exp\left(-\left(\frac{1}{\mu}+\frac{1}{\mu_0}\right)\tau(\lambda)\right), \tag{2.3.2}$$

Where $\frac{1}{\mu}+\frac{1}{\mu_0}$ is the air mass factor and $\tau(\lambda)$ is the ozone vertical optical depth (VOD) at the wavelength $\lambda$, defined as:

Preprints (www.preprints.org) | NOT PEER-REVIEWED | Posted: 23 September 2020 doi:10.20944/preprints202009.0529.v1

$$\tau(\lambda) = \int_0^\infty \sigma_{abs}(z,\lambda)\, C_{O_3}(z) dz. \quad (2.3.3)$$

Here $\sigma_{abs}(z,\lambda)$ is the ozone absorption cross-section at the height $z$ and the wavelength $\lambda$, $C_{O_3}(z)$ is the concentration of the ozone at the height $z$. Equation (2.3.3) depends on the vertical profile of $\sigma_{abs}$ and $C_{O_3}$ but in the absence of such information, we use the simplification by Kokhanovsky et al., (2020b) where the ozone optical depth is expressed as the product the total column ozone and an reference ozone absorption cross-section $\sigma_{abs,ref}(\lambda)$:

$$\tau(\lambda) = \overline{C_{O_3}}\, \sigma_{abs,ref}(\lambda)$$
$$\overline{C_{O_3}} = \int_0^\infty N(z) dz \quad (2.3.4)$$

The value of $\sigma_{abs,ref}$ was estimated by Kokhanovsky et al., (2020b) as follows. A reference vertical profile of pressure, temperature and ozone concentration was extracted from the 2D chemistry-climate model from Sinnhuber et al. (2009) at 75$^o$N and for the month of August. For these reference profiles, $\sigma_{abs}(z,\lambda)$ was calculated using the parametrization of ozone cross-section from Serdyuchenko et al. (2014), as shown in Figure 2, and integrated vertically to calculate the reference optical depth $\tau_{ref}(\lambda)$ (Eq. (2.3.3)). Eventually, the reference optical depth $\tau_{ref}(\lambda)$ was normalized by the total ozone of the reference profile, $\overline{C_{O_3}}_{ref}$= 405 DU = 8.6728e-3 kg m$^{-2}$, to derive the reference ozone absorption cross-section:

$$\sigma_{abs,ref}(\lambda) = \frac{\tau_{ref}(\lambda)}{\overline{C_{O_3}}_{ref}}. \quad (2.3.5)$$

Eventually, the transmittance can be calculated for each pixel using Equation (2.3.2) and (2.3.4):

$$T_{O_3}(\lambda) = \exp\left(-\left(\frac{1}{\mu} + \frac{1}{\mu_0}\right) \overline{C_{O_3}}\, \sigma_{abs,ref}(\lambda)\right), \quad (2.3.6)$$

Where $\overline{C_{O_3}}$ is the total column ozone concentration provided by the European Centre for Medium-Range Weather Forecast (ECMWF) within the OLCI files.

We note that one should account for the instrument spectral response function because the measurements are usually performed not at a single wavelength but in narrow spectral range $\Delta\lambda$. Therefore, the value of $\sigma_{abs,ref}(\lambda)$ will differ for different instruments even if measured at the same central wavelength.

Preprints (www.preprints.org) | NOT PEER-REVIEWED | Posted: 23 September 2020 doi:10.20944/preprints202009.0529.v1

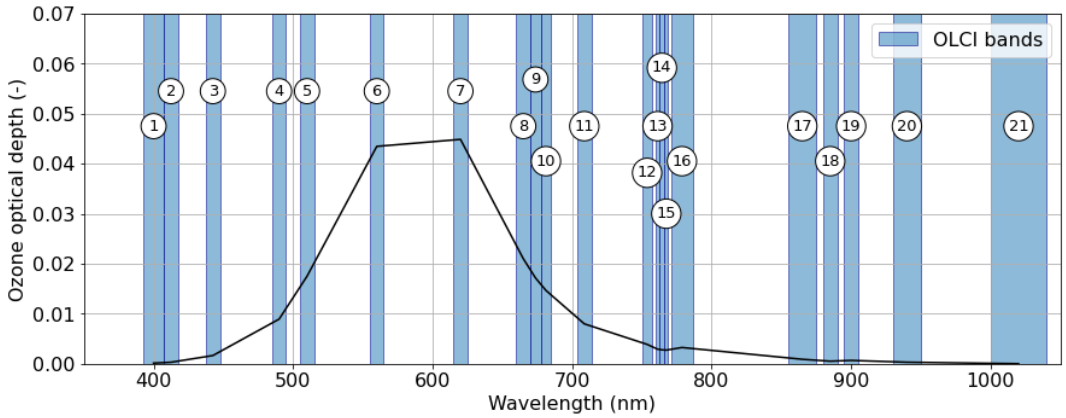


***Figure 2. Optical depth of the total ozone column as a function of wavelength. The OLCI bands are highlighted in blue.***

### 2.3.2. Molecular and aerosol scattering of light and effects on the top-of the atmosphere reflectance

The background atmospheric aerosol in Arctic is usually characterized by the low values of aerosol optical thickness and values of single scattering albedo close to one. Therefore, one can neglect light absorption by aerosol and assume that the atmosphere-underlying surface reflectance (due to molecular and aerosol scattering and reflectance from underlying surface) can be presented in the following way:

$$R_{TOA,cor\ O_3} = R_a + \frac{R_s T_a(\mu_0, \mu)}{1 - r_s r_a} \tag{2.3.7}$$

where the surface spherical albedo $r_s$ and snow reflectance $R_s$ are the quantities we want to quantify in this retrieval. But before that, three characteristics of the atmosphere need to be quantified: the atmospheric reflectance $R_a$, the spherical albedo of atmosphere $r_a$, and the total atmospheric transmittance from the top-of-atmosphere to the surface and back to the satellite $T_a(\mu_0, \mu)$.

Before the atmospheric reflectance can be derived, several characteristics of the atmosphere should be described: the molecular and aerosol optical depth, which describe how opaque the atmosphere is at a given wavelength, the phase function and its derivatives: the asymmetry parameter and backscattering fraction. In this section we describe how we derive these characteristics and eventually present the atmospheric reflectance calculation in Section***: Calculation of the atmospheric reflectance, transmittance and spherical albedo.***

Preprints (www.preprints.org) | NOT PEER-REVIEWED | Posted: 23 September 2020 doi:10.20944/preprints202009.0529.v1

***Molecular and aerosol optical depth***

The atmospheric reflectance depends on the atmospheric optical thickness, which can be presented in the following form:

$$\tau(\lambda) = \tau_{mol}(\lambda) + \tau_{aer}(\lambda) \tag{2.3.8}$$

The molecular optical depth can be approximated as

$$\tau_{mol}(\lambda) = \hat{p}\, q\, \lambda^{-\upsilon} \tag{2.3.9}$$

where $\hat{p} = \frac{p}{p_0}$, $p$ is the site pressure, $p_0 = 1013.25\, mb$, $q = 0.00877, \upsilon = 4.08$, and the wavelength is in microns. We calculate the site pressure using the following equation: $p = p_0 exp\left(-\frac{z}{H}\right)$. Here the height of the underlying surface provided in OLCI files and H = 7.64 km is the scale height.

It follows for the aerosol optical depth:

$$\tau_{aer}(\lambda) = \beta\left(\frac{\lambda}{\lambda_0}\right)^{-\alpha} \tag{2.3.10}$$

where $\lambda_0 = 0.5$ µm. The pair $(\alpha, \beta)$ represents the Angström parameters. Currently, we use the fixed values of $\alpha = 1.3\ and\ \beta = 0.1$ in our retrievals. Due to low aerosol load in Arctic, this assumption does not lead to the substantial errors.

***Phase function, asymmetry parameter and backscatter of the atmosphere***

The phase function $p(\theta)$ of a media define the light intensity scattered by the media at a given wavelength and towards the scattering angle $\theta$. The phase function is normalized so that integrating $p(\theta)$ for all $\theta$ gives one. The asymmetry parameter of the media is then defined as the intensity-weighted average cosine of the scattering angle (Hansen and Travis, 1974). It ranges from -1 for completely backscattered light to +1 for entirely forward scattered light and is defined as:

$$g = \frac{1}{2}\int_0^{\pi} p(\theta) sin\,\theta\, cos\,\theta\, d\theta \tag{2.3.11}$$

In presence of both molecular scattering and aerosol, the phase function can be presented in the following form:

Preprints (www.preprints.org) | NOT PEER-REVIEWED | Posted: 23 September 2020 doi:10.20944/preprints202009.0529.v1

$$p(\theta) = \frac{\tau_{mol} p_{mol}(\theta) + \tau_{aer} p_{aer}(\theta)}{\tau_{mol} + \tau_{aer}} \quad (2.3.12)$$

where

$$p_{mol}(\theta) = \frac{3}{4}(1 + \theta\ ) \quad (2.3.13)$$

is the molecular scattering phase function and $p_{aer}(\theta)$ is the aerosol phase function. We shall represent this function as:

$$p_{aer} = \frac{1 - {g_{aer}}^2}{(1 - 2g_{aer} cos\ \theta\ + {g_{aer}}^2)^{\frac{3}{2}}} \quad (2.3.14)$$

Therefore, it follows for the asymmetry parameter:

$$g = \frac{\tau_{aer}}{\tau_{mol} + \tau_{aer}} g_{aer} \quad (2.3.15)$$

The parameter $g_{aer}$ varies with the location, time, aerosol, type, etc. We shall assume that it can be approximated by the following equation:

$$g_{aer} = g_0 + g_1 e^{-\frac{\lambda}{\lambda_0}} \quad (2.3.16)$$

With

$$g_0 = 0.5263, g_1 = 0.4627, \lambda_0 = 0.4685 \mu m.$$

The coefficients in this equation are derived from multiple year AERONET observations over Greenland.

Another useful quantity is the so-called backscattering fraction, meaning the fraction of light scattered in the backward direction defined as:

$$B = \frac{1}{2} \int_{\frac{\pi}{2}}^{\pi} p(\theta) sin\ \theta\ d\theta \quad (2.3.17)$$

Which, using Eq. (2.3.12), translated into:

$$B = \frac{\tau_{mol} B_{mol} + \tau_{aer} B_{aer}}{\tau_{mol} + \tau_{aer}} \quad (2.3.18)$$

where $B_{mol}$ =0.5 and $B_{aer} = \frac{1-g}{2g}\left[\frac{1+g}{\sqrt{1+g^2}} - 1\right]$ (Kokhanovsky et al., 2020b).

Preprints (www.preprints.org) | NOT PEER-REVIEWED | Posted: 23 September 2020 doi:10.20944/preprints202009.0529.v1

It should be pointed that the system of equations given above enables the calculation of underlying snow-atmosphere reflectance as a function of the aerosol optical thickness for a known value of the snow spherical albedo.

***Calculation of the atmospheric reflectance, transmittance and spherical albedo***

The atmospheric reflectance $R_a$, caused by coupled aerosol-molecular scattering, can be presented within the framework of the Sobolev approximation (Sobolev, 1975) as the sum of the reflectance due to single scattering $R_{ss}$ and the reflectance due to multiple scattering $R_{ms}$:

$$R_a = R_{ss} + R_{ms} \tag{2.3.19}$$

Both contributions can be expressed as a function of the atmospheric optical depth $\tau(\lambda)$ and of the atmosphere's phase function $p(\lambda, \theta)$, and its asymmetry parameter $g(p, \lambda)$.

The single scattering contribution is expressed as:

$$R_{ss} = \frac{1 - e^{-\tau(\lambda)\,(\mu_0^{-1} + \mu^{-1})}}{4(\mu_0 + \mu)}\, p(\theta) \tag{2.3.20}$$

The multiple light scattering contribution is approximated as

$$R_{ms} = 1 + M(\tau, \mu_0, \mu) q(\mu_0, \mu) - \frac{N(\tau)}{4 + 3(1 - g)\tau} \tag{2.3.21}$$

where

$$\begin{gathered} M(\tau, \mu_0, \mu) = \frac{1 - e^{-\tau(\mu_0^{-1} + \mu^{-1})}}{4(\mu_0 + \mu)} \\ N(\tau) = f(\mu_0) f(\mu) \\ f(\mu) = 1 + \frac{3}{2}\mu + \left(1 - \frac{3}{2}\mu\right) e^{-\frac{\tau}{\mu}} \\ q(\mu_0, \mu) = 3(1 + g)\mu_0 \mu - 2(\mu_0 + \mu). \end{gathered} \tag{2.3.22}$$

The transmission function $T(\mu_0, \mu)$ is approximated as follows:

$$T(\mu_0, \mu) = e^{-B\,\tau\,(\mu_0^{-1} + \mu^{-1})} \tag{2.3.23}$$

Where *B* is the backscattering coefficient defined in Eq. (2.3.17) and Eq. (2.3.18).

The atmosphere's spherical albedo is found using the approximation proposed by Kokhanovsky et al. (2007):

Preprints (www.preprints.org) | NOT PEER-REVIEWED | Posted: 23 September 2020 doi:10.20944/preprints202009.0529.v1

$$r_a = \left(ae^{-\frac{\tau}{\alpha}} + be^{-\frac{\tau}{\beta}} + c\right)\tau \quad (2.3.24)$$

The coefficients of polynomial expansions of all coefficients (a, b, c, $\alpha, \beta$) with respect to the value of $g$ are given by Kokhanovsky et al. (2005).

## 2.4. Retrieval of the surface characteristics

### 2.4.1. Clean snow

The asymptotic radiative transfer theory relates the reflectance $R$ of a medium to its spherical albedo $r_s$ and consequently allows for the determination of spherical albedo using reflectance observations for a given observation geometry. See He and Flanner (2020) for a review of current radiative theories. The framework used here was first developed and verified with airborne measurements of albedo and reflectance over a bright cloud field with the spherical albedo in the range 0.8-0.95 (Kokhanovsky et al., 2007). This relationship was later adapted to snow by Kokhanovsky et al. (2018, 2019, 2020a) to retrieve the snow spherical albedo $r_s$ from the atmosphere-corrected OLCI reflectance $R$ as:

$$R = R_0 r_s^{\frac{u(\mu_0)u(\mu)}{R_0}}, \quad (2.4.1)$$

where $R_0$ is the theoretical reflectance of snow in the absence of absorption (Kokhanovsky et al., 2019, Appendix A), $\mu_0$ is the cosine of the solar zenith angle, $\mu$ is the cosine of the viewing zenith angle, and $u$ is the angular function (Kokhanovsky et al., 2019) defined as:

$$u(\mu_x) = \frac{3}{7}(1 + 2\mu_x) \quad (2.4.2)$$

where $\mu_x$ is either $\mu_0$ or $\mu$.

The spherical albedo for clean snow can be presented in the following form (Kokhanovsky et al, 2018):

$$r_s = \exp(-\sqrt{\alpha(\lambda) l}), \quad (2.4.3)$$

Where $l$ is the *effective absorption length* in snow and $\alpha(\lambda)$ is the bulk absorption coefficient of ice calculated from the wavelength $\lambda$ and $\chi$, the imaginary parts of ice refractive index (Warren and Brandt, 2008) reported in Section ***Appendix: Data tables used in the retrieval***:

$$\alpha(\lambda) = \frac{4\pi\,\chi(\lambda)}{\lambda}, \quad (2.4.4)$$

Preprints (www.preprints.org) | NOT PEER-REVIEWED | Posted: 23 September 2020 doi:10.20944/preprints202009.0529.v1

The plane albedo $r_p$ can be derived eventually from spherical albedo. Namely, it follows (Kokhanovsky et al., 2019):

$$r_p = r_s^{u(\mu_0)} \tag{2.4.5}$$

The effective absorption length *l does not depend* on the wavelength in the OLCI spectral range as demonstrated by Kokhanovsky et al. (2018). The same is true for $R_0$, the reflectance of non-absorbing snow layer. Therefore, we can derive both parameters from measurements of OLCI reflectance $R$ at two wavelengths $\lambda_1$ and $\lambda_2$ as in Kokhanovsky et al., (2018) that satisfy the following two criteria: i) the reflectance at these channels must be sensitive to the parameters of interest, and ii) these channels must be least influenced by atmospheric scattering and absorption processes. Consequently, the OLCI channels centred around 865 and 1020 nm are the best candidates for the retrieval.

The $R_0$ and $l$ parameters are subsequently defined as follows.

$$R_0 = R(\lambda_1)^{\frac{1}{1-\sqrt{\frac{\alpha(\lambda_1)}{\alpha(\lambda_2)}}}} R(\lambda_2)^{1-\frac{1}{1-\sqrt{\frac{\alpha(\lambda_1)}{\alpha(\lambda_2)}}}}, \tag{2.4.6}$$

And $R_0$ can then be used in Eq. (2.4.1) and (2.4.3) at the wavelength $\lambda_2$to determine $l$ :

$$l = \frac{1}{\alpha(\lambda_2)\left(\frac{u(\mu_0)u(\mu)}{R_0}\right)^2} \ln^2 \frac{R_2}{R_0} \tag{2.4.7}$$

The derived value of $l$ can be used to determine the snow spherical/plane albedo and also snow reflection function (OLCI bottom of atmosphere reflectance) at any OLCI wavelength using Eqs. (2.1.1)-(2.3.5). The diameter $d$ of ice grains in snow is estimated using the effective absorption length (Kokhanovsky et al., 2019):

$$d = Al, \tag{2.4.8}$$

where the parameter $A$ depends on the type of snow and shape of grains. We assume that *A=0.06* in the retrievals as suggested by Kokhanovsky et al. (2019). The snow specific surface area $SSA$ is derived as

$$SSA = \frac{6}{d\rho_{ice}}, \tag{2.4.9}$$

where $\rho_{ice} = 0.917$ g cm$^{-3}$ is the bulk ice density.

### 2.4.2. Polluted snow and ice

Preprints (www.preprints.org) | NOT PEER-REVIEWED | Posted: 23 September 2020 doi:10.20944/preprints202009.0529.v1

As in the case of clean snow, we assumed that scattering and absorption of light by atmosphere and impurities in snowpack can be ignored at the wavelengths 865 and 1020nm. This makes it possible to derive the parameters $R_0$, $l$, $d$ and $SSA$ in the same way as for clean snow. However, for polluted snow, $r_s$ cannot be derived from Eq. (2.4.3) because the spectral reflectance in the visible is influenced not just by ice grains but also by various impurities (soot, dust, algae).

Nevertheless, Eq. (2.3.1) describing ozone absorption, Eq. (2.3.7) describing atmospheric correction and Eq. (2.4.1) that links observed reflectance to surface reflectance and spherical albedo can still be used at all channels except those subject to molecular absorption by oxygen: channels 13-15; and water vapor: channels 19 and 20. For the remaining channels, 1-12, 16-18 and 21, Equations (2.3.1) (2.3.7) and (2.4.1) give the following system:

$$\begin{cases} R_{TOA} = \left(R_a + \dfrac{R\,T_a(\mu_0,\mu)}{1 - r_s r_a}\right) T_{O_3} \\ R = R_0 r_s^{\frac{u(\mu_0)u(\mu)}{R_0}} \end{cases} \tag{2.4.10}$$

Where $R_{TOA}$ is the measured top-of-atmosphere reflectance function, $R_a$ is atmospheric contribution to the measured signal, $r_a$ is the spherical albedo of the atmosphere, $R$ is the bottom-of-atmosphere surface reflectance, $T_a$ is atmospheric transmittance from the top-of-atmosphere to the underlying surface and back to the satellite position, $T_{O_3}$ is the transmittance of purely gaseous atmosphere. Given that $R_{TOA}$ is measured and that $R_a$, $r_a$, $T_a$, $T_{O_3}$, $R_0$ can be calculated following the approach detailed above, the system presented in Eq. (2.4.10) has therefore only one unknown, $r_s$, which cannot be presented in closed form. We consequently derive $r_s$ iteratively using Simpson's rule.

For the channels 13-15, affected by oxygen absorption, and 19-20, affected by water vapor absorption, the spherical albedos are linearly interpolated between the retrieved spherical albedo at channels 12 and 16 in the first case and channels 18 and 21 in the second.

For the very dark, polluted pixels ($R_{TOA}$<0.4 at band 21), we assume that the underlying surface is not snow, the application of the equation (2.4.6) relating the snow albedo to the snow grain size is not justified. In this case, it is assumed that the value of reflectance for a non-absorbing surface can be approximated, as discussed by Kokhanovsky et al. (2019), by the following expression:

Preprints (www.preprints.org) | NOT PEER-REVIEWED | Posted: 23 September 2020 doi:10.20944/preprints202009.0529.v1

$$R_0 = \frac{A + B(\mu_0 + \mu_0) + C\mu_0\mu + p(\theta)}{4(\mu_0 + \mu)} \quad (2.4.11)$$

where $A$ = 1.247, $B$ = 1.186, $C$ = 5.157, and

$$p(\theta) = 11.1\exp(-0.087\theta) + 1.1\exp(-0.014\theta) \quad (2.4.12)$$

and θ is the scattering angle in degrees. This formulation of $R_0$ is then used when solving Eq. (2.4.10).

***Pollutant characteristics***

The concentration of pollutants in snow is estimated using the approach described below. It is assumed that the spherical albedo, solved in Eq. (2.4.10), can also be expressed as in Kokhanovsky et al. (2018):

$$r_s = \exp\left(-\sqrt{\left(\alpha(\lambda) + \frac{k_{abs}(\lambda)}{B_{ice}c_s}\right)l}\right) \quad (2.4.13)$$

where $k_{abs}(\lambda)$ is spectral absorption coefficient of impurities, $B_{ice}$ is so-called absorption enhancement parameter for ice grains (Kokhanovsky et al., 2019), $c_s$ is the volumetric concentration of ice grains in snowpack and α(λ) is the bulk absorption coefficient of ice defined in Eq. (2.4.4). We shall assume that $B_{abs}$=*1.6* in the retrieval procedure.

In the visible spectrum, the absorption by ice particle can be neglected ($\alpha(\lambda) \approx 0$) and the polluted snow spherical albedo can be presented in the following form:

$$r_s(\lambda) = \exp\left(-\sqrt{\frac{k_{abs}(\lambda)}{B_{ice}c_s}}l\right) \quad (2.4.14)$$

or

$$k_{abs}(\lambda) = B_{ice}\, c_s\, \frac{\ln^2\left(r_s(\lambda)\right)}{l}$$

Let us assume that the impurity absorption coefficient $k_{abs}(\lambda)$ can also be expressed in following form:

$$k_{abs}(\lambda) = k_{abs}(\lambda_0)\left(\frac{\lambda}{\lambda_0}\right)^{-m} \quad (2.4.15)$$

where $\lambda_0 = 1\mu m$. The Angström absorption coefficient $m$ can then be derived from Eq. (2.4.14) and (2.4.15) evaluated at $\lambda_1 = 400$ nm and , $\lambda_2 = 412.5$ nm where the spherical albedo $r_s$ was previously derived:

Preprints (www.preprints.org) | NOT PEER-REVIEWED | Posted: 23 September 2020 doi:10.20944/preprints202009.0529.v1

$$m = \frac{\ln\left(\frac{\ln^2(r_s(\lambda_1))}{\ln^2(r_s(\lambda_2))}\right)}{\ln\left(\frac{\lambda_2}{\lambda_1}\right)} \quad (2.4.16)$$

The Angström coefficient can then be used to characterize the type of pollutant present in the snow. Since soot has a typical Angström coefficient around one while dust's Angström coefficient ranges from 3 to 7, we here assume that the snow is polluted by black carbon if $m$ < 1.2 and by dust pollution otherwise.

Eq. (2.4.15) evaluated for $\lambda_1$ also gives:

$$k_{abs}(\lambda_0) = \left(\frac{\lambda_1}{\lambda_0}\right)^m \frac{\ln^2(r_s(\lambda_1))}{l}. \quad (2.4.17)$$

Eq. (2.4.13) can be used to derive $k_{abs,n}(\lambda)$, the normalized absorption coefficient of impurities:

$$k_{abs,n}(\lambda) = \frac{k_{abs}(\lambda)}{c_s} = B_{abs}\left(\frac{\ln^2(r_s(\lambda))}{l} - \alpha(\lambda)\right) \quad (2.4.18)$$

Once again, neglecting absorption by ice particle from the measurements at the wavelength $\lambda_1 = 400$ nm ($\alpha(\lambda_1) \approx 0$), the relative volumetric concentration of pollutants in snow $c$ can be derived:

$$c = \frac{c_p}{c_s} = \frac{B_{ice}\ \ln^2(r_s(\lambda_1))}{K(\lambda_1)l} \quad (2.4.19)$$

where $K(\lambda) = k_{abs}(\lambda)/c_p$ is the volumetric absorption coefficient of impurities.

In the case of soot, $K(\lambda)$ can be approximated as in Kokhanovsky et al., (2018):

$$K(\lambda) = B_{soot}\ \alpha_s(\lambda). \quad (2.4.20)$$

Here, $B_{soot}$ is the enhancement $\alpha_s(\lambda) = \frac{4\pi}{\lambda}\chi_s(\lambda)$ is the bulk absorption coefficient of soot , $\chi_s(\lambda)$ is the imaginary part of soot refractive index, currently set at a constant 0.47.

In the case of dust pollution, we assume: $K(\lambda_1) = 0.01\mu m^{-1}$ to calculate the relative volumetric concentration of pollutants in snow $c$.

## 2.5. Broadband albedo calculation

### 2.5.1. General case

Preprints (www.preprints.org) | NOT PEER-REVIEWED | Posted: 23 September 2020 doi:10.20944/preprints202009.0529.v1

The derived spectral albedo is used to integrate the planar and spherical broadband albedo (BBA) $\bar{r}_{p,s}(\lambda_1, \lambda_2)$ over any wavelength interval $[\lambda_1, \lambda_2]$:

$$\bar{r}_{p,s}(\lambda_1, \lambda_2) = \frac{\int_{\lambda_1}^{\lambda_2} r_{p,s}(\lambda) F(\lambda)\, d\lambda}{\int_{\lambda_1}^{\lambda_2} F(\lambda) d\lambda} \tag{2.5.1}$$

where $F(\lambda)$ is the incident solar flux at the snow surface, $r_{p,s}(\lambda)$ is plane ($p$) or spherical ($s$) albedo depending plane or spherical BBA, $\bar{r}_{p,s}(\lambda_1, \lambda_2)$, is to be calculated. Currently, only shortwave spherical/plane BBA ($\lambda_1 = 300$ nm, $\lambda_2 = 2400$ nm) is being retrieved but additional ranges may be added in the future depending on user demand.

Broadband albedo are only weakly sensitive to the variation of $F(\lambda)$. The spectrum of incident solar flux at the snow surface is therefore assumed to be identical in all pixels and is approximated by the following analytical equation:

$$F(\lambda) = p_0 + p_1 e^{-\beta \lambda} + p_2 e^{-\gamma \lambda} \tag{2.5.2}$$

where $p_0 = 3.238\text{e+}1$, $p_1 = \text{-}1.6014033\text{e+}5$, $p_2 = 7.95953\text{e+}3$, $\beta = 11.71$ μm$^{-1}$, and $\gamma = 2.48$ μm$^{-1}$. The coefficients have been derived using the code SBDART (Ricchiazzi et al., 1998) in the spectral range 300-2400 nm at the following assumptions.

***Table 3. Assumptions used in SBDART to derive the solar flux at the surface***

| Parameter | Value |
|---|---|
| water vapor column | 2.085 g m$^{-2}$ |
| ozone column | 0.35 atm-cm |
| tropospheric ozone | 0.0346 atm-cm |
| aerosol model | rural (Shettle and Fenn, 1979) |
| vertical optical depth of boundary layer at 550nm | 0.1 |
| altitude | 825 m a.s.l. |
| solar zenith angle | 60 degrees |
| snow albedo at the surface | calculated using spherical grains of 0.25 mm diameter |

### 2.5.1. Approximation used for clean snow

In the case of clean snow, the exact integration of BBA (Eq. (2.3.14)) is possible because the spectral reflectance is known for each of OLCI measurement wavelength. However, this integration is time consuming. To speed up the retrieval process, the shortwave spherical albedo can be directly expressed as a function of the retrieved grain diameter:

Preprints (www.preprints.org) | NOT PEER-REVIEWED | Posted: 23 September 2020 doi:10.20944/preprints202009.0529.v1

$$\bar{r}_s(\lambda_1, \lambda_2) = a + b \exp\left(-\frac{d}{\Delta}\right) + c \exp\left(-\frac{d}{\gamma}\right) \quad (2.5.3)$$

where $d$ is expressed in microns and a = 0.642, b = 0.1044, c = 0.1773, $\beta$ = 158.62 µm, and $\gamma$ = 2448.18 µm.

For the shortwave broadband plane albedo, we use the same equation as for the spherical albedo. However, the second order polynomial is used to represent the dependence of the coefficients $a$,$b$,$c$, $\Delta$ , $\gamma$ with respect to the cosine of the solar zenith angle $\mu_0$: $a = \varepsilon_a + \varsigma_a \mu_0 + \eta_a \mu_0^2$, $b = \varepsilon_b + \varsigma_b \mu_0 + \eta_b \mu_0^2$ … etc. The coefficients of parametrization are given in Table 4.

***Table 4. The coefficients of the parametrization for the shortwave plane albedo.***

| | $\varepsilon$ | $\varsigma$ | $\eta$ |
|---|---|---|---|
| a | 0.7389 | -0.1783 | 0.0484 |
| b | 0.0853 | 0.0414 | -0.0127 |
| c | 0.1384 | 0.0762 | -0.0268 |
| $\Delta$, microns | 187.89 | -69.2636 | 40.4821 |
| $\gamma$, microns | 2687.25 | -405.09 | 94.5 |

### 2.5.2. Approximation used for polluted snow and ice

For polluted snow, the spherical albedo $r_s$ and planar albedo $r_p$ cannot be expressed in a closed form as it is the solution of the system of equation (2.4.10). Nevertheless, $r_{p,s}$ ($r_s$ and $r_p$ respectively) are known for each of the wavelength corresponding to OLCI channels. To circumvent this issue, we build functions of the wavelength that approximate the retrieved $r_{p,s}$ over three intervals:

1) Over 400-709 nm, we approximate spherical and planar albedo $r_{p,s}$ by a polynomial of the second order fitted to the retrieved $r_{p,s}(\lambda = 400$ nm), $r_{p,s}(\lambda = 560$ nm), and $r_{p,s}(\lambda = 709$ nm).

2) Over 709-865 nm, we approximate spherical and planar albedo $r_{p,s}$ by a polynomial of the second order fitted to the retrieved $r_{p,s}(\lambda = 709$ nm), $r_{p,s}(\lambda = 753$ nm), and $r_{p,s}(\lambda = 865$ nm).

3) Over 865-2400 nm, we approximate the spherical and planar albedo $r_{p,s}$ with an exponential function fitted to the retrieved $r_{p,s}(\lambda = 865$ nm), and $r_{p,s}(\lambda = 1020$nm).

Preprints (www.preprints.org) | NOT PEER-REVIEWED | Posted: 23 September 2020 doi:10.20944/preprints202009.0529.v1

These assumptions make it possible to derive the value of BBA analytically.

First, for all three intervals, the denominator of Eq. (2.5.1) can be calculated as:

$$\int_{\lambda_1}^{\lambda_2} F(\lambda)d\lambda = \int_{\lambda_1}^{\lambda_2} p_0 + p_1 e^{-\frac{\lambda}{\lambda_1}} + p_2 e^{-\frac{\lambda}{\lambda_2}}\, d\lambda$$
$$= p_0\,(\lambda_2 - \lambda_1) + p_1 \frac{e^{-\beta\lambda_1} - e^{-\beta\lambda_2}}{\beta} + p_2 \frac{e^{-\gamma\lambda_1} - e^{-\gamma\lambda_2}}{\gamma}, \quad (2.5.4)$$

Over the intervals $[\lambda_1, \lambda_2]$, either equal to 400-709 nm or 709-865 nm, the spherical albedo can be expressed using its polynomial approximation:

$$r_{p,s} = c\lambda^2 + b\lambda + a \quad (2.5.5)$$

Where a, b and c take different values whether they are fitted to derived $r_p$ or $r_s$. With this formulation of $r_s$, the numerator in Eq. (2.5.1) can be expressed in the following form:

$$\int_{\lambda_1}^{\lambda_2} r_{p,s}(\lambda)F(\lambda)\,d\lambda = a + bK(\lambda_1, \lambda_2) + cL\,(\lambda_1, \lambda_2) \quad (2.5.6)$$

where

$$K(\lambda_1, \lambda_2) = p_0\,(\lambda_2^2 - \lambda_1^2)/2$$
$$+p_1\left[\left(\frac{1}{\beta^2} + \frac{\lambda_1}{\beta}\right)e^{-\beta\lambda_1} - \left(\frac{1}{\beta^2} + \frac{\lambda_2}{\beta}\right)e^{-\beta\lambda_2}\right] \quad (2.5.7)$$
$$+p_2\left[\left(\frac{1}{\gamma^2} + \frac{\lambda_1}{\gamma}\right)e^{-\gamma\lambda_1} - \left(\frac{1}{\gamma^2} + \frac{\lambda_2}{\gamma}\right)e^{-\gamma\lambda_2}\right],$$

And

$$L(\lambda_1, \lambda_2) = p_0(\lambda_2^3 - \lambda_1^3)/3$$
$$+p_1\left[\left(\frac{2}{\beta^3} + \frac{2\lambda_1}{\beta^2} + \frac{\lambda_1^2}{\beta}\right)e^{-\beta\lambda_1} - \left(\frac{2}{\beta^3} + \frac{2\lambda_2}{\beta^2} + \frac{\lambda_2^2}{\beta}\right)e^{-\beta\lambda_2}\right] \quad (2.5.8)$$
$$+p_2\left[\left(\frac{2}{\gamma^3} + \frac{2\lambda_1}{\gamma^2} + \frac{\lambda_1^2}{\gamma}\right)e^{-\gamma\lambda_1} - \left(\frac{2}{\gamma^3} + \frac{2\lambda_2}{\gamma^2} + \frac{\lambda_2^2}{\gamma}\right)e^{-\gamma\lambda_2}\right].$$

For wavelengths in the 865-2400 nm range, we use the exponential approximation of $r_{p,s}$:

$$r_{p,s} = \sigma \exp(-\epsilon\lambda) \quad (2.5.9)$$

Where $\sigma$ and $\epsilon$ take different values whether they are fitted to derived $r_p$ or $r_s$. And in that case, the numerator in Eq. (2.5.1) can be expressed in the following form:

Preprints (www.preprints.org) | NOT PEER-REVIEWED | Posted: 23 September 2020 doi:10.20944/preprints202009.0529.v1

$$\int_{\lambda_1}^{\lambda_2} r_{p,s}(\lambda)F(\lambda)\,d\lambda = \sigma(p_0 i_0(\epsilon) + p_1 i_0(\epsilon+\beta) + p_2 i_0(\epsilon+\gamma) \quad (2.5.10)$$

## 3. NDSI and NDBI

The normalized difference snow index (NDSI) is calculated as:

$$NDSI = \frac{R(865nm) - R(1020nm)}{R(865nm) + R(1020nm)}. \quad (2.5.1)$$

A pixel is considered snow-covered if NDSI is in the range 0.3-0.4 and R(400nm) is larger than 0.75. The normalized difference bare ice index (NDBI) is calculated as:

$$NDBI = \frac{R(400nm) - R(1020nm)}{R(400nm) + R(1020nm)}. \quad (2.5.2)$$

The bare ice is classified in two steps. First, dark bare ice is identified where NDBI is less than 0.65 and R (400nm) is less than 0.75. Then for cases the dark bare ice flag is not set, the bare ice flag is equal to one (100% bare ice – covered pixel), if NDSI is larger than 0.33. Also is assumed that the dark dirty bare ice flag is equal to one (100% dark dirty bare ice – covered pixel), if NDBI is smaller than 0.65 and R (400nm) is smaller than 0.75 and that a land mask is used.

## 4. Appendix: Data tables used in the retrieval

***Table A 1. The ozone vertical optical thickness ($\tau_{ozone}$) as function of wavelength λ in terrestrial atmosphere at the ozone concentration of 405 DU = 8.6728e-3* kg m$^{-2}$.**

| λ (nm) | $\tau_{ozone}$ (-) | λ (nm) | $\tau_{ozone}$ (-) | λ (nm) | $\tau_{ozone}$ (-) |
|---|---|---|---|---|---|
| 400 | 1.38E-04 | 665 | 2.10E-02 | 767.5 | 2.73E-03 |
| 412.5 | 3.05E-04 | 673.75 | 1.72E-02 | 778.75 | 3.26E-03 |
| 442.5 | 1.65E-03 | 681.25 | 1.47E-02 | 865 | 8.96E-04 |
| 490 | 8.94E-03 | 708.75 | 7.98E-03 | 885 | 5.19E-04 |
| 510 | 1.75E-02 | 753.75 | 3.88E-03 | 900 | 6.72E-04 |
| 560 | 4.35E-02 | 761.25 | 2.92E-03 | 940 | 3.13E-04 |
| 620 | 4.49E-02 | 764.375 | 2.79E-03 | 1020 | 1.41E-05 |

***Table A 2. The imaginary part χ of ice refractive index at OLCI bands and wavelength (λ) as reported in Warren and Brandt (2008).***

| Band | λ (nm) | χ | Band | λ (nm) | χ | Band | λ (nm) | χ |
|---|---|---|---|---|---|---|---|---|
| Oa1 | 400 | 2.37E-11 | Oa8 | 665 | 1.78E-08 | Oa15 | 767 | 8.13E-08 |

| | | | | | | | | |
|---|---|---|---|---|---|---|---|---|
| Oa2 | 412 | 2.70E-11 | Oa9 | 673 | 1.95E-08 | Oa16 | 778 | 9.88E-08 |
| Oa3 | 442 | 7.00E-11 | Oa10 | 681 | 2.10E-08 | Oa17 | 865 | 2.40E-07 |
| Oa4 | 490 | 4.17E-10 | Oa11 | 708 | 3.30E-08 | Oa18 | 885 | 3.64E-07 |
| Oa5 | 510 | 8.04E-10 | Oa12 | 753 | 6.23E-08 | Oa19 | 900 | 4.20E-07 |
| Oa6 | 560 | 2.84E-09 | Oa13 | 761 | 7.10E-08 | Oa20 | 940 | 5.53E-07 |
| Oa7 | 620 | 8.58E-09 | Oa14 | 764 | 7.68E-08 | Oa21 | 1020 | 2.25E-06 |

## References

Doherty, S. J., Warren, S. G., Grenfell, T. C., Clarke, A. D. and Brandt, R. E.: Light-absorbing impurities in Arctic snow, Atmos. Chem. Phys., 10(23), 11647–11680, doi:10.5194/acp-10-11647-2010, 2010.

Hansen, J. E. and Travis, L. D.: Light scattering in planetary atmospheres, Space Sci. Rev., 16(4), 527–610, doi:10.1007/BF00168069, 1974.

He, C. and Flanner, M.: Snow Albedo and Radiative Transfer: Theory, Modeling, and Parameterization, Springer International Publishing., 2020.

Hudson, S. R., Warren, S. G., Brandt, R. E., Grenfell, T. C. and Six, D.: Spectral bidirectional reflectance of Antarctic snow: Measurements and parameterization, J. Geophys. Res. Atmos., 111(18), D18106, doi:10.1029/2006JD007290, 2006.

Kokhanovsky, A., Mayer, B., Von Hoyningen-Huene, W., Schmidt, S. and Pilewskie, P.: Retrieval of cloud spherical albedo from top-of-atmosphere reflectance measurements performed at a single observation angle, Atmos. Chem. Phys., 7(13), 3633–3637, doi:10.5194/acp-7-3633-2007, 2007.

Kokhanovsky, A., Lamare, M., Di Mauro, B., Picard, G., Arnaud, L., Dumont, M., Tuzet, F., Brockmann, C. and Box, J. E.: On the reflectance spectroscopy of snow, Cryosphere, 12(7), 2371–2382, doi:10.5194/tc-12-2371-2018, 2018.

Kokhanovsky, A., Lamare, M., Danne, O., Brockmann, C., Dumont, M., Picard, G., Arnaud, L., Favier, V., Jourdain, B., Meur, E. Le, Di Mauro, B., Aoki, T., Niwano, M., Rozanov, V., Korkin, S., Kipfstuhl, S., Freitag, J., Hoerhold, M., Zuhr, A., Vladimirova, D., Faber, A. K., Steen-Larsen, H. C., Wahl, S., Andersen, J. K., Vandecrux, B., van As, D., Mankoff, K. D., Kern, M., Zege, E. and Box, J. E.: Retrieval of snow properties from the Sentinel-3 Ocean and Land Colour Instrument, Remote Sens., 11(19), 1–49, doi:10.3390/rs11192280, 2019.

Kokhanovsky, A., Box, J. E., Vandecrux, B., Mankoff, K. D., Lamare, M., Smirnov, A. and Kern, M.: The determination of snow albedo from satellite measurements using fast atmospheric correction technique, Remote Sens., 12(2), 1–18, doi:10.3390/rs12020234, 2020a.

Kokhanovsky, A. A., Mayer, B. and Rozanov, V. V.: A parameterization of the diffuse transmittance and reflectance for aerosol remote sensing problems, Atmos. Res., 73(1–2), 37–43, doi:10.1016/j.atmosres.2004.07.004, 2005.

Kokhanovsky, A. A., Lamare, M. and Rozanov, V.: Retrieval of the total ozone over snow fields using Sentinel-3 Ocean and Land Colour Instrument, 2020b.

Proksch, M., Rutter, N., Fierz, C. and Schneebeli, M.: Intercomparison of snow density measurements: Bias, precision, and vertical resolution, Cryosphere, 10(1), 371–384, doi:10.5194/tc-10-371-2016, 2016.

Ricchiazzi, P., Yang, S., Gautier, C. and Sowle, D.: SBDART: A Research and Teaching Software Tool for Plane-Parallel Radiative Transfer in the Earth's Atmosphere, Bull. Am. Meteorol. Soc., 79(10), 2101–2114, doi:10.1175/1520-0477(1998)079<2101:SARATS>2.0.CO;2, 1998.

Rozanov, V. V. and Rozanov, A. V.: Differential optical absorption spectroscopy (DOAS) and air mass factor concept for a multiply scattering vertically inhomogeneous medium: Theoretical consideration, Atmos. Meas. Tech., 3(3), 751–780, doi:10.5194/amt-3-751-2010, 2010.

Serdyuchenko, A., Gorshelev, V., Weber, M., Chehade, W. and Burrows, J. P.: High spectral resolution ozone

 doi:10.20944/preprints202009.0529.v1

absorption cross-sections – Part 2: Temperature dependence, Atmos. Meas. Tech., 7(2), 625–636, doi:10.5194/amt-7-625-2014, 2014.

Shettle, E. P. and Fenn, R. W.: Models for the Aerosols of the Lower Atmosphere and the Effects of Humidity Variations on their Optical Properties, 1979.

Sinnhuber, B. M., Sheode, N., Sinnhuber, M., Chipperfield, M. P. and Feng, W.: The contribution of anthropogenic bromine emissions to past stratospheric ozone trends: A modelling study, Atmos. Chem. Phys., 9(8), 2863–2871, doi:10.5194/acp-9-2863-2009, 2009.

Skiles, S. M. K., Flanner, M., Cook, J. M., Dumont, M. and Painter, T. H.: Radiative forcing by light-absorbing particles in snow, Nat. Clim. Chang., 8(11), 964–971, doi:10.1038/s41558-018-0296-5, 2018.

Sobolev, V. V.: Light scattering in planetary atmospheres, Pergamon Press., 1975.

Warren, S. G.: Can black carbon in snow be detected by remote sensing?, J. Geophys. Res. Atmos., 118(2), 779–786, doi:10.1029/2012JD018476, 2013.

Warren, S. G. and Brandt, R. E.: Optical constants of ice from the ultraviolet to the microwave: A revised compilation, J. Geophys. Res. Atmos., 113(14), D14220, doi:10.1029/2007JD009744, 2008.